Pergamon

PII: S0191-8141(96)00071-5

Journal of Structural Geology, Vol. 18, No. 12, pp. 1381 to 1388, 1996

0191-8141/96 $15.00 + 0.00

Implications of structural segmentation during earthquakes: the 1995 Egion earthquake, Gulf of Corinth, Greece

I. K. KOUKOUVELAS and T. T. DOUTSOS

Department of Geology, University of Patras, Patras, 26110 Greece

(*Received* 28 *November* 1995; *accepted in revised form* 15 *August* 1996)

Abstract—The Egion earthquake which occurred in the Gulf of Corinth, central Greece ($Ms = 6.2$) on 15 June 1995 was caused by normal slip on the north-dipping and WNW-trending Egion fault. The Egion fault ruptured at depth during the Egion mainshock and probably re-ruptured at shallow level during the largest aftershock. The surface trace of the Egion fault has a segmented geometry. Linkage between three segments, which show long-term deformation differences as well as coseismic segmentation, enabled all segments to be incorporated in an earthquake segment. The surface ruptures continued to grow after the coseismic motion; the afterslip throw of the fault 10 weeks after the main event was equal to the 3 cm value for maximum coseismic slip. This afterslip was accompanied by uplift of the footwall block and a warp-like hangingwall subsidence (folding). This pattern of deformation was associated with more complex deformation at the western end of the earthquake segment. Here, afterslip was accompanied by general subsidence of the whole area (between 25th June and 30th July), followed by uplift of the whole area without afterslip (between 30th July and 2nd September). The afterslip-rate averaged over the 73 day period after the main event varied from 0.48 mm day^{-1} along the central part of the earthquake segment to 0.16 mm day^{-1} at the eastern end of the earthquake segment. Copyright © 1996 Elsevier Science Ltd

INTRODUCTION

On 15 June 1995, a large earthquake ($Ms = 6.2$, National Observatory of Athens), hereafter called the Egion earthquake, occurred in the vicinity of Egion in the Corinthian Gulf. The Egion earthquake was accompanied 15 minutes later by the largest aftershock ($M_L = 5.4$) and spatially localized activity (Tselentis *et al.* 1996). Source parameters for the Egion earthquake suggest that the reactivated fault has a length of rupture $r = 6.7$ km, average displacement at depth $u = 0.85$ m, and seismic moment $Mo = 5.7 \times 10^{25}$ dyne cm (Stavrakakis & Chouliaras in press).

The Gulf of Corinth is a 130 km long seismic belt within the extensional region of the Aegean (Fig. 1a). This seismic belt is undergoing N–S extension with much of this extension accommodated by earthquakes hosted by WNW- and ENE-trending, 10–40 km long normal faults in the upper crust (Jackson *et al.* 1982, King *et al.* 1985, Ambraseys & Jackson 1990, Doutsos & Piper 1990, Jackson 1994, Roberts & Koukouvelas 1996). These faults define the southern side of the asymmetric Corinth half-graben (Brooks & Ferentinos 1984, offshore data, and Doutsos & Poulimenos 1992 onshore data). Earthquakes related with this extension occur in discrete spatial groupings, i.e. in the Egion–Akrata and Corinthos areas (Fig. 1b). The spatial groupings correspond to the east (Corinthos area) and the west (Egion area) terminations of the Corinth graben. Records of historical seismicity close to the Egion area show that four large earthquakes (Papazachos & Papazachou 1989, Mouyaris *et al.* 1992) have occurred in the 2261 years before 1888 AD, the date of the latest great earthquake that destroyed Egion town.

Five major north-facing WNW-trending normal faults that are segmented along their strikes at the surface are present on the southern flank of the Gulf of Corinth in the Egion area (Fig. 2). Rupture segments were produced along the Eliki fault during the 1861 earthquake (Fig. 2). This segmentation was mapped (Schmidt 1879) within the bedrock-cored footwall block. The Eliki fault is characterized by a dome-shaped uplifted footwall block and a half-spoon shaped subsiding hanging-wall basin (Roberts & Koukouvelas 1996). The boundary between the two ruptured segments during the 1861 earthquake also coincided with major changes in gross morphology showing that this boundary (Fig. 2, south of Eliki) marks a persistent segment boundary which can be named as a 'salient' using in a broad sense the definitions by Machette *et al.* (1991). Fault segmentation along all faults indicates that this is the dominant fault geometry in the area. Segmentation on various scales along fault traces has been recently recognized as a fundamental property of faults. This recent recognition that many faults are segmented in map view, in cross-section, in terms of earthquake activity as well as in laboratory experiments has implications for how incremental deformation takes place in faults (Tchalenko 1970, Aki 1979, Schwartz & Coppersmith 1984, Sibson 1986, Cowie & Scholz 1992, Dawers & Anders 1995, Willemse *et al.* 1996).

In this paper we present a map of the surface ruptures produced during the 1995 earthquake sequence as well as geodetic records of the post-seismic deformation, and consider how this fits into the pattern of long-term deformation of the region. Furthermore, by integrating structural data and earthquake information data we discuss the near-field deformation that took place during the onset of the Egion fault seismic cycle.

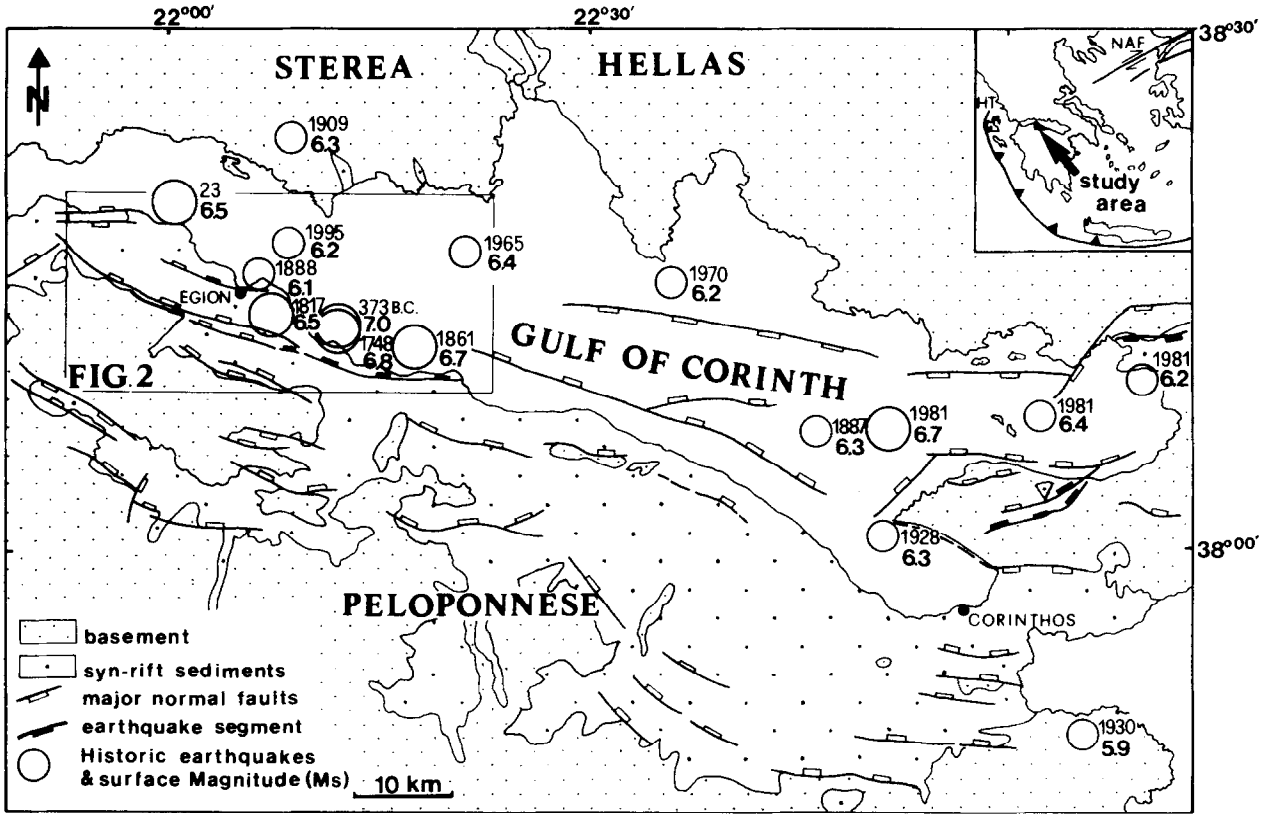

Fig. 1. Tectonic map (after Koukouvelas *et al.* 1996) of the Gulf of Corinth showing active faults, syn-rift sediments, and historical earthquakes (seismic data after Papazachos & Papazachou 1989, Ambraseys & Jackson 1990). Inset shows the geotectonic position of the study area. HT, Hellenic trench, NAF, North Anatolian fault.

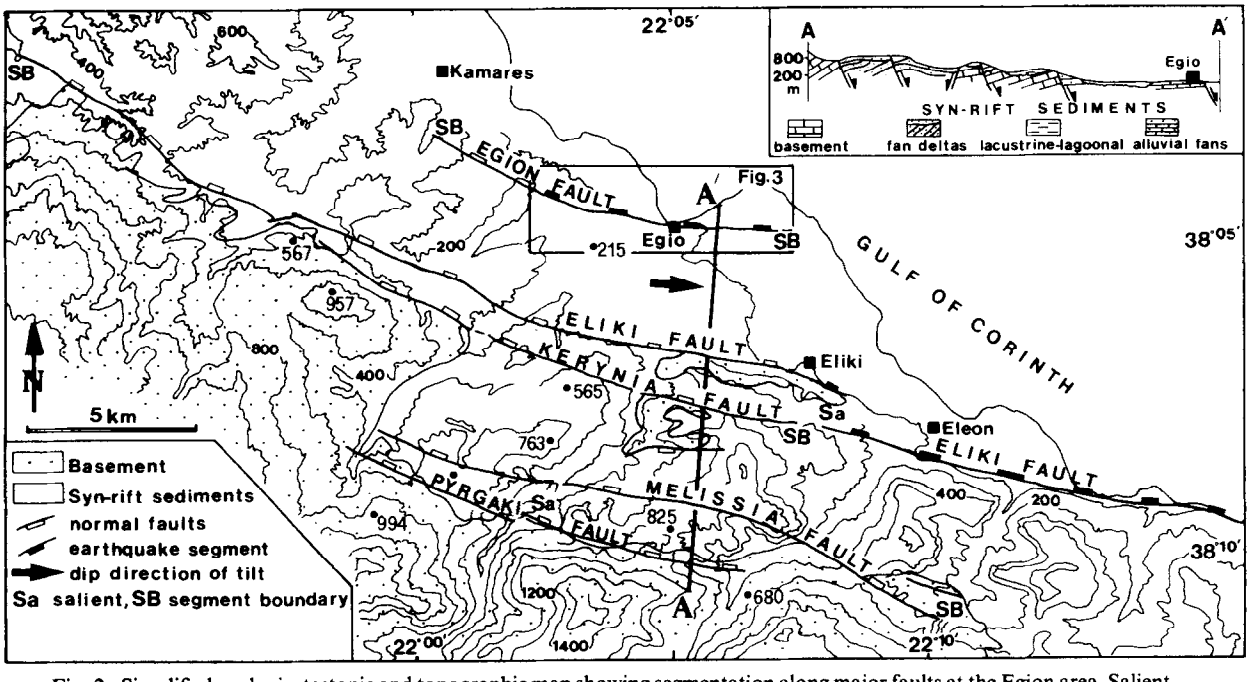

Fig. 2. Simplified geologic, tectonic and topographic map showing segmentation along major faults at the Egion area. Salient along Eliki fault is defined following the nomenclature of Machette *et al.* (1991). Earthquake segment along Eliki fault after Schmidt (1879).

DATA PRESENTATION

Structural segmentation of the Egion fault

The 12 km long Egion fault (Fig. 2) was reactivated during the 1995 earthquakes by surface ruptures. A geomorphological escarpment and monoclinal warps mark the position of the fault, forming a hill-front along the coast of the gulf, suggesting that the fault controls the uplift of the built-up area of Egion. Three structural or geometric segments can be defined along the Egion fault. The 2.2 km long Stafidalona fault segment (Fig. 3) that trends WNW–ESE is expressed on the surface as a monocline on the alluvial plane within the cultivated area around Stafidalona, upthrowing the SSE block of the studied area (Fig. 3). The top of this monocline was ruptured during the earthquake. No evidence of a fault escarpment has been observed along this fault segment. The 2 km long E–W trending Egion fault segment forms a clear fault escarpment 40–100 m high and is offset from the Stafidalona segment by a zone of diffuse deformation. The slope angle of this fault escarpment has an average value of 37 °, a value that is close to the repose angle of the sediments (G. Koukis 1995, personal communication), suggesting repeated activation of the involved fault (Koukouvelas *et al.* 1996). Geological estimates of the total geological offset of the fault segment (defined by sediment thickness, height of fault scarp and erosion) indicate that this segment has a maximum throw of 200 m (Doutsos & Poulimenos 1992) that diminishes along strike. A ENE-trending fault is the boundary between Egion and Agios Konstantinos segments (Fig. 3b). The 8 km long WNW-trending Agios Konstantinos fault segment crosses a hilly area and dies out south of Kamares village (Fig. 2). West of the village, the fault scarp completely loses its topographic expression in a deep valley. The total throw of this fault segment is about 45 m.

Time averaged slip rates for vertical movement, during the last 1.8 Ma, for segmented faults south of Egion town (Fig. 2) have been calculated by Doutsos & Poulimenos (1992) with values between 0.16–0.76 mm a^{-1}; the basin-filling architecture of the Egion area is controlled by activity on these faults (Poulimenos 1993, Dart *et al.* 1994). The Eliki and Egion faults, flanking the Gulf of Corinth shoreline, control the points of entry of alluvial sediments, causing the river courses to bend to the southeast (i.e. bend of Meganitas river, Fig. 3) towards areas of high hangingwall subsidence, and ultimately the present day gulf (Roberts & Jackson 1991). These two faults lie 3–4 km apart and the overlapping eastern termination of the Egion fault with the Eliki fault forms an east-tilted basin floor (see arrow in Fig. 2). This tilted surface was a basin floor during the Pleistocene, acting as an active submarine depocenter that is now elevated 100 m above sea level; its sediments are now being cannibalized and redeposited within the Gulf of Corinth. The present day depocenter has been structurally shifted to the north to lie around 300 m below sea level (Ferentinos 1995, personal communication).

Surface ruptures during the last earthquake

The epicentral area of the Egion earthquake is in obvious structural proximity with the Eliki fault (Fig. 1). Surface ruptures as well as macroseismic data for the Eliki fault have been linked to two historical earthquakes and so at first, it was suspected that the Eliki fault trace may have been ruptured by the earthquake. However, no evidence of surface ruptures, warping, soil slides or macroseismic effects were found along the Eliki fault.

Surface ruptures produced during the 1995 earthquake

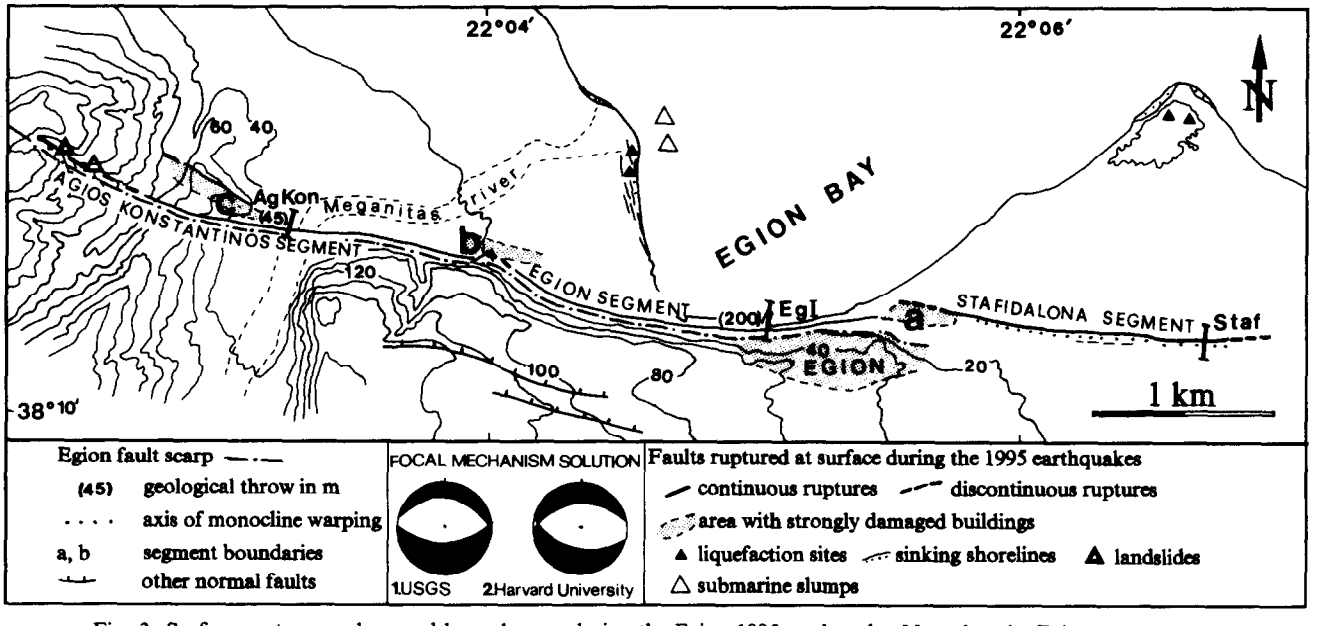

Fig. 3. Surface ruptures and ground hazards map during the Egion 1995 earthquake. Note that the Egion segment was entirely ruptured while the Stafidalona and Agios Konstantinos segments were partly ruptured. Focal mechanism solution is shown as lower-hemisphere equal-area projection.

sequence occurred along the eastern part of the 12 km-long Egion fault and were found 7 hours after the mainshock (Fig. 2). However the mapping of those ruptures was complete 27 hours after the mainshock, a time period in which several large aftershocks were recorded. The total length of surface ruptures on the Egion fault was about 7.2 km. Surface ruptures occurred along the eastern portion of Agios Konstantinos segment, the entire length of the Egion segment, and much of the Stafidalona segment (Fig. 3). From east to west the earthquake scarps are:

Stafidalona segment (length (L) = 2.2 km; maximum coseismic displacement (D_{cmax}) = 1.5 cm). The maximum coseismic displacement is directly measured as the maximum throw observed on each segment.

Egion segment (L = 2 km; D_{cmax} = 3 cm)

Agios Konstantinos segment (L = 3 km; D_{cmax} = 2.5 cm). The cross-strike distances between the echelon steps of the rupture range from 80 to 150 m (Fig. 3, locations a & b). At (a), a series of five fractures was observed on asphalt roads with no vertical motion; at (b) we mapped a ENE-trending ground crack where all displacements were parallel to the ground surface, producing open cracks < 1 cm across. All the surface ruptures are accompanied by warp-like hangingwall subsidence (folding) in a zone of about 20–25 m wide. Also, at one site along the Agios Konstantinos segment the warped area was dislocated by an antithetic surface rupture with a 2 cm throw.

The Stafidalona surface rupture was observed in a cultivated area as a continuous rupture that broke across irrigation canals. Despite the maximum values for coseismic displacement of 1.5 cm for the Stafidalona segment quoted above, elsewhere at Stafidalona village, the rupture was observed after the earthquake as a ground crack with all displacement parallel to the ground surface. However, two months after the main earthquake, measurements of the same fracture indicated a throw of 1 cm. The fracture along the Egion fault segment was observed 20–60 m to the north of the 40 to 100 metre high fault escarpment and also suffered similar afterslip (sensu Sylvester 1986) increasing the 3 cm value for coseismic displacement to 5.7 cm after a two month period. The fracture along the Agios Konstantinos fault segment was more complex exhibiting an E–W trending linear rupture that divided into two branches close to the Agios Konstantinos village (Fig. 3, AgKon). The north branch dies out as a system of ground cracks with no throw while the south branch dies out in a deep valley in which rock fall and soil slides were triggered by the earthquake. Afterslip of the southern fracture has also been observed, increasing the coseismic throw by 2.5 cm to a value of 3.5 cm after two months. All of this afterslip was coincident with a period of aftershock activity as described below.

GEODETIC MEASUREMENTS

Installing topographic arrays — data

Immediately after the surface ruptures were mapped (we started mapping surface ruptures on June 15 and finished one day later) three sites for establishing topographic arrays (nails on asphalt or irrigation canals) were established during June 17 (Table 1). These three sites are located at the center (Egion embarkation dock, nails on asphalt road), at the eastern end (Stafidalona area, nails on irrigation canals) and at western end (Agios Konstantinos village, nails on asphalt road) of the ruptures (Fig. 3). These arrays range in length from 110 to 145 m, are nearly perpendicular to the rupture and contain from 8 to 13 nails.

We used two series of instruments; an electronic geodetic station and an automatic level specification instrument with strut-supported Invar leveling rods. With this equipment it is possible to measure with a precision of 2 mm for elevation specifications and 2 ± 1 mm for horizontal distances. Ground compaction errors are probably negligible as the roads and canals were built 25 years ago. Subsequent surveys (Fig. 4) of these profiles were surveyed early in the morning in order to avoid refractive index errors due to temperature increase during the day. Refraction errors are due to the optical method of observation with refraction affected by pressure, temperature, latitude, humidity etc. Most of these parameters were nearly stable during the survey. In all sites we measured deflection to one arbitrarily fixed point located as far as possible from the fault trace. The first survey along each array was carried out immediately after the installation, 17th June, and the re-surveying dates were 18 and 25 June, 30 July, and 2 September. The first survey was carried out in order to establish a datum. This datum corresponds in Fig. 4 with the x-axis, also showing the sites of the nails.

Table 1. Fault-crossing networks

Location/designation	Marks	Orientation of survey-line	Monitored motions	Number of nails and length of survey lines	Frequency of resurvey
Agios Konstantinos AgKon	nails in asphalt	NNE	vertical leveling height changes	13/145	days to months
Egion main dock EgI	nails in asphalt	N–S	vertical leveling height changes	8/110	days to months
Stafidalona Staf	nails in concrete	NNW	vertical leveling height changes	10/130	days to months

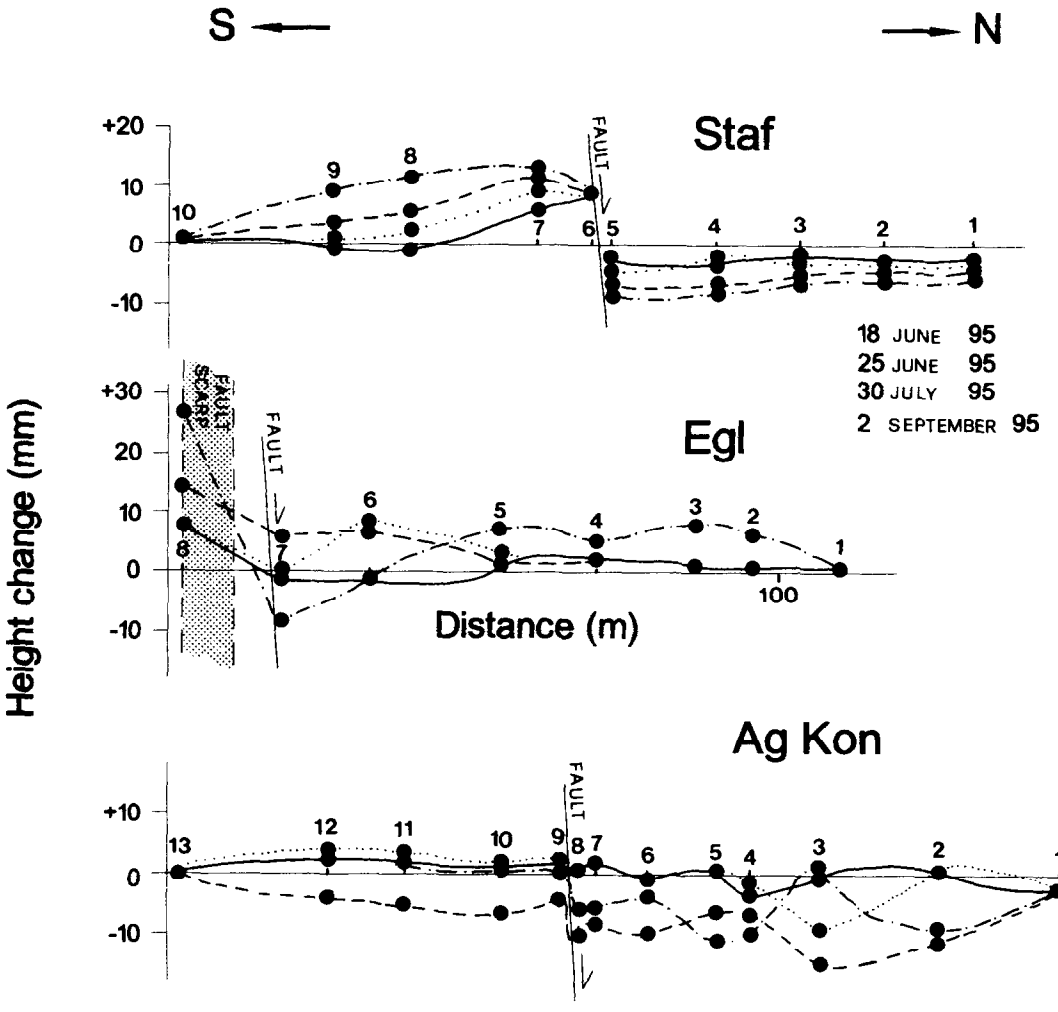

Fig. 4. Height change across three line-surveys across the rupture trace, indicated in Fig. 3. Nail 1 is arbitrarily held constant in EgI. Nails 10 and 13 are arbitrarily held constant for Staf and AgKon sites respectively. EgI: embarkation dock at Egion, Staf: Stafidalona cultivated area, and AgKon: asphalt road in Agios Konstantinos village.

Results

The survey period included nine aftershocks with local magnitude (M_L) greater than 4.0 and was marked by a hyperbolic decrease in the number of smaller events each day (Tselentis *et al.* 1996). This distribution indicates that a period of eighteen days is probably enough to lead the Egion earthquake rupture zone into the period of post-seismic quiescence (sensu Scholz 1988).

In the Stafidalona segment we measured a continuous uplift of the footwall block and subsidence of the hangingwall block during the survey period (Fig. 4a). The measured afterslip throw at the eastern end of the earthquake segment indicates a uniform (through time) and continuous footwall uplift, totalling 12 mm, and hangingwall subsidence, totalling 8 mm. This deformation (Fig. 4 profile Staf) is similar to the deformation style associated with the surface ruptures of the Borah Peak earthquake (Stein & Barrientos 1985). For this eastern area we calculate, for a time period of 73 days, a slip rate of 0.16 mm day^{-1}.

On the Egion segment we measured continuous uplift of the footwall block (Fig. 4b). The hanging-wall shows general subsidence during the survey period interrupted by a period of uplift between 25th June and 30th July. The survey of 18th June showed height changes in one day, and thus the measured footwall uplift of 8 mm is the fastest rate of uplift during our surveying period. This rate of uplift was measured during the third day after the main event, in the central part of the earthquake segment (Fig. 4, profile EgI, nail 8 relative to nail 7). At the same site we recorded in the two month surveying period, total footwall uplift of 27 mm and a maximum hangingwall subsidence of 8 mm (Fig. 4, profile EgI, nail 8 relative to nail 7). Based on these two numbers we estimate the permanent deformation (uplift and subsidence) as 35 mm. Thus we calculate the slip rate for a period of 73 days at 0.48 mm day^{-1}. The highest tectonic relief on the Egion fault occurs in this area (Fig. 3).

The western end of the earthquake segment exhibited a rather complex deformation divided into two periods, one showing a general subsidence of both fault blocks (Fig. 4, profile AgKon, 30 July '95), that was later superposed upon by a general uplift of area without increase in throw and subsidence of nail 4 (Fig. 4, profile AgKon, 2 September '95). Although the analysis of this superposition, or the relationships between these two periods of deformation is beyond the scope of this work

we believe that this subsidence is perhaps related to a release of pre-seismic deformation. At the area of Agios Konstantinos, pre-seismic deformation was recorded as uplift of the ground surface in the yard of a house and anomalous discharge from Mantilo spring (personal communication with local people)(Fig. 3c). The slip rate ratio for this area for a period of 73 days is not defined as the deformation is very complex and will be dealt with in another paper.

All these data indicate that the footwall uplift along the earthquake segment reaches its maximum at the central part of the fault where co-seismic throw is higher and decreases at the tip lines where co-seismic throw is reduced. By comparing these data with the geologic offsets along the same fault scarp we testify that the afterslip and the long-term deformation are similar.

DISCUSSION

The quantitative afterslip data and post-seismic slip rate for the Egion fault are the first records of this type for a seismogenic fault in the Aegean region. Although the Egion fault is a relatively small fault, this study provides a basis for studying the pattern of deformation and seismic hazard in central Greece. The Egion fault is easily assessable while surface ruptures were mapped a few hours after the earthquake. Therefore, the uncertainties in rupture length and vertical throw are in practice negligible. Furthermore, geological data has been reconciled with seismological data and a model suggested for the growth of the Egion seismogenic fault.

Origin of surface ruptures

Two lines of evidence indicate that surface ruptures were broadly coeval with the earthquake: (a) the 7.2 km-long surface ruptures during the 1995 earthquake are straight in map view and cut inland across coastal deltas. This surface rupture length produced by the Egion earthquake ($Ms = 6.2$) fits well onto the regression line which relates length parameters with earthquake size (Wells & Coppersmith 1994); (b) throw along these straight ruptures mimics the geological throw along the Egion fault (Fig. 3). Liquefaction phenomena in this area are well known (Schmidt 1879), and this study has revealed an acurate pattern of ground ruptures which follow the coast, more than 400 m north of straight co-seismic ruptures. So surface ruptures (Fig. 3) are related to co-seismic fault motion at depth rather than liquefaction.

Comparison of seismological and geological data

Source parameters (data after USGS, Harvard University, Stavrakakis & Chouliaras in press) are fairly similar to the surface data reported here.

In addition to these data, microseismical data at the Egion area, collected during August 1991, and related focal mechanism solutions indicate that microearthquakes at the Egion area are hosted on north dipping fault planes (Rigo 1994). These faults in practice control the evolution of the Gulf of Corinth (Brooks & Ferentinos 1984, Higgs 1988, Doutsos & Poulimenos 1992) (Fig. 2). Furthermore Rigo's (1994) epicenters show intensive earthquake activity at an area near to that reactivated during the Egion 1995 mainshock and consequent aftershocks (see also Stavrakakis & Chouliaras in press and Tselentis *et al.* 1996).

Slip-vectors, associated with the Egion earthquake ruptures, converging towards the hanging-wall (Roberts & Koukouvelas 1996), are similar to those reported by Jackson *et al.* (1982) for the active faults which produced the 1981 Corinthian earthquakes that were related with motions at depth.

Circumstantial evidence suggests the surface fault was active prior to the Egion earthquake. Local surface movement was suggested by a pre-seismic uplift which developed in a house at the Agios Konstantinos village two months prior to the Egion earthquake. This house is located 30 m north of the co-seismic surface rupture at the Agios Konstantinos village. Following the Egion earthquake, three ground cracks sub-parallel to the main surface rupture traversed the property with a spacing of 4–5 m, all corresponding to the axis of the uplift. At the same geographic location anomalous spring discharge was observed immediately after the earthquake, as quoted above. Although phenomena related to an impending earthquake is very difficult to evaluate (Scholz 1988,1990) this evidence may be connected with microearthquake activity of the Egion area that was instrumentally recorded, as a cluster of small magnitude earthquakes prior the Egion mainshock.

Significance of afterslip

Afterslip growing on a surface fault is a fundamental physical process following coseismic offset at depth (Marone *et al.* 1991). The development of afterslip on faults is directly related with the upward propagation of the coseismic slip during the aftershock activity (Doser & Kanamori 1986, Marone & Scholz 1988). The afterslip observations made here on the Egion fault that are correlated with the aftershock activity suggest that motions at depth are correlated with the afterslip on the surface. Thus the aftershock 15 min after the mainshock at a 1.2 km depth may have re-ruptured the Egion fault at a depth which corresponds to the transition from poorly consolidated rocks to basement; with the aftershock activity restricted probably to the basement. From the above it is inferred that the down dip prolongation of the Egion fault may have hosted the Egion mainshock. In our interpretation, which coincides partly with Tselentis *et al.* (1996), the M 5.4 aftershock increased the throw of the surface ruptures, but as an afterslip effect. However, a more detailed analysis of the coseismic offset and afterslip creep can be fitted by inversion techniques but it is not our intention to discuss them further here.

Implications of co-seismic and afterslip segmentation

The Egion earthquake ruptured a portion of the 12 km-long Egion fault. Surface ruptures during the earthquake achieved a length of 7.2 km and are divided into three segments. Each segment is characterized by a different co-seismic vertical throw and afterslip. As co-seismic segmentation mimics the segmentation of the Egion fault it is inferred that the Egion fault maintains a self-similar displacement profile and structure through time. Thus we suggest that the Egion fault is growing by segment linkage (sensu Segall & Pollard 1980, Peacock & Sanderson 1991, Cartwright *et al.* 1995).

CONCLUSIONS

(1) Long-term deformation, coseismic throw and afterslip deformation on the Egion fault shows a segmented pattern of deformation with the segments showing large geologic offset coincident with areas of high coseismic and afterslip throw.

(2) Subsequent surveys for two months after the main event across the Egion 1995 earthquake segment show the following types of deformation: the central part of the earthquake segment is characterized by a high slip rate of 0.48 mm day^{-1}; At the eastern part of the earthquake segment the slip rate ratio is reduced to 0.16 mm day^{-1}; the western end is characterized by superposition of two discrete deformation processes, subsidence and uplift, and thus it is difficult to estimate the total uplift or subsidence.

(3) Afterslip (including both uplift and subsidence) that occurred in the 73 days following the main earthquake doubled the coseismic slip.

(4) Processes involved in Egion fault growth fall into the model of 'growth by segment linkage'.

Acknowledgements—We thank Prof. A. Papadimitriou for assistance in installing the geodetic arrays and L. Stamatelatos for surveying assistance. We also thanks G. Poulimenos for assistance in the field. The editing assistance of R. J. Lisle, and reviews by G. P. Roberts, P. Burton and D. J. W. Piper led to valuable improvements in the text.

REFERENCES

Aki, K. 1979. Characterization of barriers on an earthquake fault. *J. geophys. Res.* **84**, 6140–6148.

Ambraseys, N. N. & Jackson, J. A. 1990. Seismicity and associated strain of central Greece between 1890 and 1988. *Geophys. J. Int.* **101**, 663–708.

Brooks, M. & Ferentinos, G. 1984. Tectonics and sedimentation in the Gulf of Corinth and the Zakynthos and Kefallinia channels, western Greece. *Tectonophysics* **101**, 25–54.

Cartwright, J. A., Trudgill, B. D. & Mansfield, C. S. 1995. Fault growth by segment linkage: an explanation for scatter in maximum displacement and trace length data from the Canyonlands Grabens of SE Utah. *J. Struct. Geol.* **17**, 1319–1326.

Cowie, P. A. & Scholz, C. H. 1992. Physical explanation for the displacement–length relationship of faults using a post-yield fracture mechanics model. *J. Struct. Geol.* **14**, 1133–1148.

Dart, C. J., Collier, R. E., Gawthorpe, R. L., Keller, J. V. & Nichols, G. 1994. Sequence stratigraphy of (?) Pliocene–Quaternary synrift, Gilbert-type fan deltas, northern Peloponnesos, Greece. *Mar. Petrol. Geol.* **11**, 545–560.

Dawers, N. H. & Anders, M. H. 1995. Displacement–length scaling and fault linkage. *J. Struct. Geol.* **17**, 607–614.

Doser, D. I. & Kanamori, H. 1986. Depth of seismicity in the Imperial Valley region 1977–1983 and its relationship to heat flow, crustal structure, and the October 15, 1979, earthquake. *J. geophys. Res.* **91**, 675–688.

Doutsos, T. & Piper, D. J. W. 1990. Listric faulting, sedimentation and morphological evolution of the Quaternary eastern Corinth rift, Greece: First stages of continental rifting. *Bull. geol. Soc. Am.* **102**, 812–829.

Doutsos, T. & Poulimenos, G. 1992. Geometry and kinematics of active faults and their seismotectonic significance in the western Corinth–Patras rift (Greece). *J. Struct. Geol.* **14**, 689–699.

Higgs, B. 1988. Syn-sedimentary structural controls on basin deformation in the Gulf of Corinth, Greece. *Basin Res.* **1**, 155–165.

Jackson, J. A. 1994. Active Tectonics of the Aegean Region. *Ann. Rev. Earth Planet. Sci.* **22**, 239–271.

Jackson, J. A., Gagnepain, J., Houseman, G., King, G. C. P., Papadimitriou, P., Soufleris, C. & Vireux, J. 1982. Seismicity and the geomorphological development of the Gulf of Corinth (Greece): the Corinth earthquakes of February and March 1981. *Earth Planet. Sci. Lett.* **57**, 377–397.

King, G. C. P., Ouyang, Z. X., Papadimitriou, P., Deschamps, A., Gagnepain, L., Houseman, G., Jackson, J. A., Soufleris, C. & Virieux, J. 1985. The evolution of the Gulf of Corinth (Greece); an aftershock study of the 1981 earthquakes. *Geophys. J. R. Astron. Soc.* **80**, 677–693.

Koukouvelas, I., Mpresiakas, A., Sokos, E. & Doutsos, T. 1996. The tectonic setting and earthquake ground hazards of the 1993 Pyrgos earthquake, Peloponnese, Greece. *J. geol. Soc. Lond.* **152**, 39–49.

Machette, M. N., Personius, S. F., Nelson, A. R., Schwartz, D. P. & Lund, W. R. 1991. The Wasatch fault zone, Utah-segmentation and history of Holocene earthquakes. *J. Struct. Geol.* **13**, 137–149.

Marone, C. & Scholz, C. H. 1988. The depth of seismic faulting and the upper transition from stable to unstable slip regimes. *Geophys. Res. Lett.* **15**, 621–624.

Marone, C. J., Scholtz, C. H. & Bilham, R. 1991. On the mechanics of earthquake afterslip. *J. geophys. Res.* **96**, 8441–8452.

Mouyaris, N., Papanastasiou, D. & Vita-Finzi, C. 1992. The Helice Fault? *Terra Nova* **4**, 124–129.

Papazachos, B. C. & Papazachou, K. 1989. *Earthquakes in Greece*. Ziti Publications.

Peacock, D. C. P. & Sanderson, D. J. 1991. Displacements, segment linkage and relay ramps in normal fault zones. *J. Struct. Geol.* **13**, 721–733.

Poulimenos, G. 1993. Tectonics and sedimentation in the western Corinth graben. *Neus. Jb. geol. Palaont. Mh.* **10**, 607–630.

Rigo, A. 1994. Etude seismotectonique et geodesique du golfe de Corinthe (Greece). These dc Doctorat de l' Universite Paris VII.

Roberts, G. P. & Koukouvelas, I. 1996. Structural and seismological segmentation of the Gulf of Corinth fault system: implications for models of fault growth. *Ann. Geophys.* **39**, 619–646.

Roberts, S. & Jackson, J. A. 1991. Active normal faulting in central Greece: an overview. In: *The Geometry of Normal Faults* (edited by Roberts, A. M., Yielding, G. & Freeman B.). *Spec. Publ. geol. Soc. Lond.* 56, 125–142.

Schmidt, J. 1879. Studien uber Erdbeben, Alwin Georgi, Leipzig, 68–83

Scholz, C. H. 1988. Mechanisms of Seismic Quiescences. *Pure Appl. Geophys.* **126**, 701–718.

Scholz, C. H. 1990. *The Mechanics of Earthquakes and Faulting*. Cambridge University Press.

Schwartz, D. P. & Coppersmith, K. 1984. Fault behavior and characteristic earthquakes: examples from the Wasatch and San Andreas fault zones. *J. geophys. Res.* **89**, 5681–5689.

Segall, P. & Pollard, D. D. 1980. Mechanics of discontinuous faults. *J. geophys. Res.* **85**, 4337–4350.

Sibson, R. H. 1986. Rupture interaction with fault jogs. In: *Earthquake Source Mechanics* (edited by Das, S., Boatwright, J. & Scholz, C.). *Am. Geophys. Un. Geophys. Monogr., Maurice Ewing Series* **6**, 157–167.

Stavrakakis, G. N. & Chouliaras, G. In press. Source parameters of the Arnea, Kozani and Aigion earthquakes based on digital data. In: *Proceedings of Congress XV: Seismicity of the Carpatho–Balkan Region, Carpatho–Balkan Geol. Ass.*

Stein, R. S. & Barrientos, S. E. 1985. Planar high-angle faulting in the Basin and Range: geodetic analysis of the 1983 Borah Peak, Idaho, earthquake. *J. geophys. Res.* **90**, 11355–11366.

Sylvester, A. G. 1986. Near-Field Tectonic Geodesy. In: *Active Tectonics* (edited by Wallace, R. E.). National Academic Press, Washington, 164–180.

Tchalenko, J. S. 1970. Similarities between shear zones of different magnitudes. *Bull. geol. Soc. Am.* **81**, 1625–1640.

Tselentis, G-A., Melis, N. S., Sokos, E. & Papatsimpa, K. 1996. The Egion June 15, 1995 (6.2 M_L) Earthquake, Western Greece. *Pure Appl. Geophys.* **147**, 83–98.

Wells, D. L. & Coppersmith, K. J. 1994. New empirical relationships among magnitude, rupture length, rupture width, rupture area, and surface displacement. *Bull. Seism. Soc. Am.* **84**, 974–1002.

Willemse, E. J. M., Pollard, D. D. & Aydin, A. 1996. Three-dimensional analyses of slip distributions on normal fault arrays with consequences for fault scaling. *J. Struct. Geol.* **18**, 295–309.